ANALYSIS AND DESIGN OF GRID-CONNECTED PHOTOVOLTAIC SYSTEMS WITH MULTIPLE-INTEGRATED CONVERTERS OF MPPT TECHNIQUES

Asst.Prof. R. Praveen kumar M.E, M.B.A.
prawinbaskar@gmail.com

Mr. T. Arvinthraj, Mr. M.Mathivana Prabu
Mr. V. Moorthy, Mr. R. Nandha Kumar

Department of Electrical and Electronics Engineering
AVS Engineering College Salem.

Abstract**—**In this paper describes the architecture of multiple-integrated converter modules sharing an unfolding full-bridge inverter with a pseudo dc link (MIPs) is proposed for grid-connected photovoltaic systems in this paper. The proposed configuration can improve the power conversion, the control circuit complexity, and the cost competitiveness. The proposed MIP is composed of distributed flyback dc–dc converters (DFCs) and an unfolding full-bridge inverter with an ac filter. The DFCs can eliminate the shading effect by using the individual maximum power point tracking. In conventional flyback-type single-phase utility-interactive inverters, discontinuous conduction mode and boundary conduction mode are popular because of the inherent constant current-source characteristics more desirable for grid connection and of the simple procedures for the controller design. However, the operating mode suffers from a large current stress of the circuit components, which leads to the low power efficiency. To avoid this, the DFCs operate under continuous conduction mode that allows reduced current stresses and increased power efficiency, as well as low material cost. The current control loop of the converters employs primary-side regulation contributing to improvement of dynamics as well as the cost reduction significantly due to the elimination of the high-linearity photo coupler device. Development of a new dc-current loop that maintains the level of dc-current injection into the grid within the levels stipulated will be dealt as well. The performance validation of the proposed design is confirmed byexperimental results.

Keywords**—** DC-DC power converter, maximum power point tracker, Nonlinear control systems, photovoltaic system

I.INTRODUCTION

PHOTOVOLTAIC (PV) systems are a suitable option toproduce clean electrical energy since they can be dimensioned for a wide range of power ratings in both stand-alone and grid-connected applications [1], [2]. A typical PV system is composed by a PV array, a dc/dc converter to transform the power provided by the PV source, and an inverter, as depicted in Fig. 1. The PV array is characterized by a nonlinear behavior that changes significantly with the operating condition e.g., irradiance level, shades, temperature, among others, which makes difficult to predict the voltage and current to guarantee maximum power production [3]. The operation point in which the PV array provides its maximum power is named maximum power point (MPP) [4], [5]. Then, the main objective of the control strategy in a PV system is to ensure the system operation around its MPP (maximum power point tracking—MPPT) in whichever load and environmental conditions [3]–[6]. In the literature, the most commonly used MPPT solutions are the incremental conductance and the perturb and observe (P&O) [7], where the P&O is widely adopted due to its simple implementation and tracking efficiency [4], [8]. The connection between the dc/dc converter and the inverter causes voltage oscillations since the power delivered by the PV panel is dc and the power injected by the inverter is ac [9], [10]. If such oscillations are not well mitigated, the PV power delivered to the grid may be affected, also making difficult the tracking of the MPP by the MPPT algorithm [4]. To face this problem, an electrolytic capacitor is connected between the dc/dc converter and the inverter, as illustrated in Fig. 1, but such a solution decreases the reliability of the system [11]. Many solutions have been proposed to mitigate such oscillations.

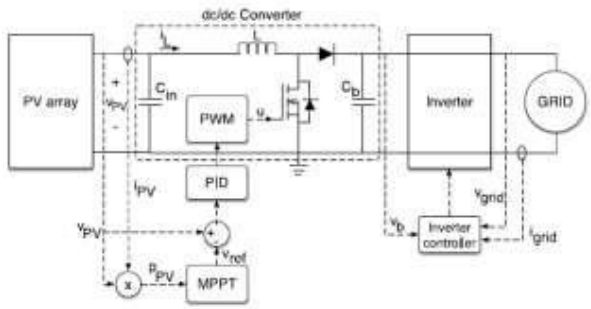

Fig. 1. PV system scheme based on classical PID controller.

II. BACKGROUND OF THE PROPOSED DESIGN PROCEDURE

In this paper, small-signal analysis and design guidelines of a MIP with a CCM flyback converter and an unfolding full bridge inverter have been proposed. A desirable feature of the work is the material-cost reduction from a new architecture of the dc-link multi module structure with the current and from a new analog-circuited dc-rejection controller. From the small-signal analysis, the transfer functions derived by state-space averaging method are verified by comparison between the exact switching model and the averaged model. Then, the analysis and design guidelines have been verified through the experimental test of a hardware prototype of the MIP. For experimental verification, an average-current-mode controller with the primary switch current has been implemented. The entire system's power efficiency was 90% at the maximum and greater than 86% in overall range. The analog-circuited MPPT performance of the hardware prototype was mostly over 99%. Another issue is dc-current injection. To overcome the problem, a dc-rejection circuit that introduces a current reference waveform based on measurement of the dc component at grid current has been proposed. As a result, a dc-rejection circuit is applied to the MIP circuit, using costly persuasive devices. The proposed scheme achieves an acceptable dc-current level at the output of the MPPT system.

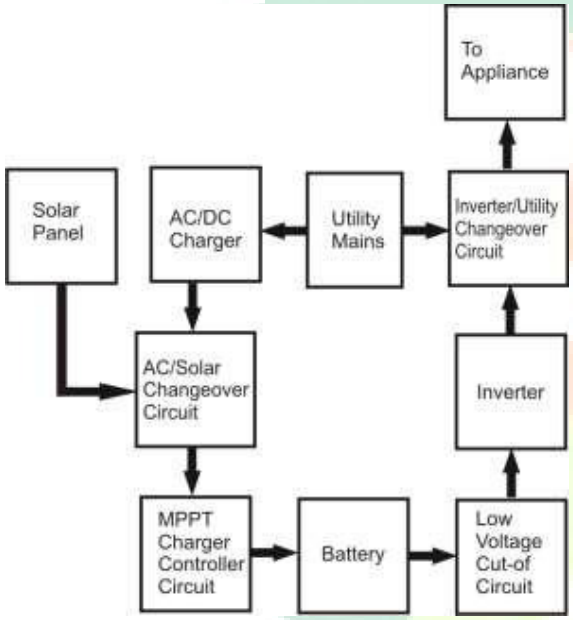

Proposed Block Diagram

A. Solar Panel

A photovoltaic (in short PV) module is a packaged, connected assembly of typically 6×10 solar cells. Solar Photovoltaic panels constitute the solar array of a photovoltaic system that generates and supplies solar electricity in commercial and residential applications. Each module is rated by its DC output power under standard test conditions, and typically ranges from 100 to 365 watts. The efficiency of a module determines the area of a module given the same rated output – an 8% efficient 230 watt module will have twice the area of a 16% efficient 230 watt module. There are a few solar panels available that are exceeding 19% efficiency. A single solar module can produce only a limited amount of power; most installations contain multiple modules. A photovoltaic system typically includes a panel or an array of solar modules, a solar inverter, and sometimes a battery and/or solar tracker and interconnection wiring.

B. Inverter

An inverter is an electric apparatus that changes direct current (DC) to alternating current (AC). It is not the same thing as an alternator, which converts mechanical energy (e.g. movement) into alternating current.

Direct current is created by devices such as batteries and solar panels. When connected, an inverter allows these devices to provide electric power for small household devices. The inverter does this through a complex process of electrical adjustment. From this process, AC electric power is produced. This form of electricity can be used to power an electric light, a microwave oven, or some other electric machine.An inverter usually also increases the voltage. In order to increase the voltage, the current must be decreased, so an

inverter will use a lot of current on the DC side when only a small amount is being used on the AC side. Inverters are made in many different sizes. They can be as small as 150 watts, or as large as 1 megawatt

C. Battery

An electric **battery** is a device consisting of two or more electrochemical cells that convert stored chemical energy into electrical energy. Each cell has a positive terminal, or cathode, and a negative terminal, or anode. The terminal marked positive is at a higher electrical potential energy than is the terminal marked negative. The terminal marked negative is the source of electrons that when connected to an external circuit will flow and deliver energy to an external device. When a battery is connected to an external circuit,electrolytes are able to move as ions within, allowing the chemical reactions to be completed at the separate terminals and so deliver energy to the external circuit. It is the movement of those ions within the battery which allows current to flow out of the battery to perform work. [1] Although the term *battery* technically means a device with multiple cells, single cells are also popularly called batteries. Primary (single-use or "disposable") batteries are used once and discarded; the electrode materials are irreversibly changed during discharge. Common examples are the alkaline battery used for flashlights devices.

III ANALYSIS

Based on the previous section, it is required to design a process for the SMC that ensures the system stability, the desired settling time, and null overshoot. Therefore, such a design process must to take into account all the elements in the control loops, e.g., requirements of the MPPT algorithm, SMC, filters, etc. A good alternative to define the behavior of the PV voltage vPV is to include both the error with respect to the reference and the voltage derivative into the switching function, where the voltage derivative can be acquired by measuring the input capacitor current iCin . The main advantage of such a switching function concerns the regulation of the PV voltage without additional controllers based on linearized models. Therefore, this paper is based on the switching function Ψ and surface Φ given in (6), which enable to analyze the stability of the PV voltage in presence of load, environment, or reference Changes.It must be pointed out that such a switching function Ψ is similar to the one adopted in [20], i.e., equivalent switching function (5). However, this paper is focused in providing a new analysis and design procedure for the control system, without including any of the simplifications adopted in [20], to guarantee a stable behavior of the SMC and a correct tracking of the MPPT. The scheme presented in Fig. 4(a) is used to implement the switching function Ψ, where the voltage reference v_{ref} is provided by a P&O controller. The dynamic behavior of the dc/dc converter is modeled by (7) and (8), where i_{PV} and v_b represent the PV current and the bulk voltage, respectively, while the manipulated variable u corresponds to the activation signal of the semiconductor switches.The PVcurrent can be modeled by the simplified single-diode model (9) [20], [22], where iSC represents the short-circuit current, IR is the diode saturation current, and α represents the thermal voltage that depends on the array temperature [20]. The parameters of this model can be calculated from the operation condition and datasheet values as described in [22], where the Short-circuit current is approximately proportional to the irradiance.

A.Transversality Condition

The transversality condition (10) guarantees that the manipulated variable u is present in the switching function derivative [14], which is required to modify the system dynamics To verify condition (10), the derivative of the function Ψ with respect to the time is obtained in (11) and the derivative of the PV current is given.

B. Equivalent Control Condition

The next step is to analyze the equivalent control condition, which imposes that the average value u_{eq} of the control variable u must be constrained within the operation range of that control variable [24]. For the dc/dc converter, the correct range is $0 < u_{\text{eq}} < 1$.

C.Reachability Conditions\

The reachability conditions analyze the ability of the system to reach the desired state Ψ = 0. The work in [24] demonstrated that a system that fulfills the equivalent control condition also fulfills the reachability conditions. The work also shows that the sign of the transversality condition imposes the value of u for each reachability condition. Due to the implementation constraints, which are discussed in Section IV, the proposed design of the SMC requires a negative value for the parameter $K2$. Hence, the transversality condition in (14) is positive, which imposes the reachability conditions (23) and (24) provided that the control action is implemented as $u = 1$for $\Psi < 0$ and $u = 0$.Then, the reachability conditions are calculated by evaluating (13) in (23) and (24), obtaining (25) and (26). By replacing (17) in (25) and (26), the same inequalities given in (19) and (20) as shown on the bottom of the next page are obtained. Therefore, ensuring that dv_{ref}/dt is constrained within the dynamic limits given in (21) and (22) as shown bottom of the page also grants that both reachability conditions are fulfilled.

IV. CONTROLLER IMPLEMENTATION

This paper uses hysteresis comparators for implementing the SMC, which is a common practice for dc/dc converter applications. Moreover, an hysteresis band H must be added to the sliding surface to limit the switching frequency [14], hence the surface is constrained within $-H2 \leq \Psi \leq H2$. From such a condition inequalities (23) and (24) are implemented as in (27), whose electrical scheme is presented in Fig. 6. Its practical realization was performed using a TS555 integrated circuit, which exhibits the same internal structure. The conditions for u in (27) are defined by the positive sign of the transversality condition (14), it requiting a negative value of $K2$, which also imposes a negative value to $K1$. Adopting positive values for $K1$ and $K2$ will require additional implementation circuitry.

A. *Switching Frequency Analysis*

The SMC implementation based on hysteresis comparators imposes a variable switching frequency $f$sw . Taking into account that the input capacitor and the inductor of the scheme in Fig. 5 form a second-order filter [25] and due to the small-ripple condition of the PV voltage, the magnitude of the current ripples for both the inductor iL and the capacitor iCin is the same [25], i.e., iCin = iL . Then, the switching frequency $f$sw imposed by the SMC is calculated from the derivative of the inductor current (8) and the duty cycle of the boost converter as in (28). Such an expression can be used to define i_{Cin} in agreement with the practical limitations of the switching frequency imposed by the semiconductors and sensors.

B. *Calculation of K_2*

The SMCs are commonly implemented using commercial circuits, e.g., the TS555 and operational amplifiers, H must be chosen according to the operation range of those components. Moreover, i_{Cin} must be designed to guarantee continuous conduction mode and to avoid large ripples in the PV voltage. In addition, as point out in (28), i_{Cin} must be also defined in agreement with the practical limitations of the switching frequency.

C. *Design of the Reference Filter*

The first step to design the low-pass filter added in Fig. 5 for the voltage reference is to define the filter order. Such a topic was addressed in [20] by using a first-order filter designed as in (30), which avoids overshoots in the reference delivered to the SMC and exhibits a settling time equal to $t_{s,1st} = 3.9 \cdot \tau_f$ However, using a second-order filter, it is possible to obtain the same performance with a shorter settling time, which is desirable to enable shorter T_a values to improve the MPPT tracking speed. Therefore, this paper adopts the second-order filter given in (31), which considers a damping ratio $\zeta = 1$ to avoid overshoots in the reference of the SMC.

D. *Summary of the Design Procedure*

The design of the SMC is based on the requirements of the P&O algorithm used to perform the MPPT: Perturbation magnitude v_{MPPT} and period T_a . Moreover, practical constraints must be also considered, e.g., maximum switching frequency, maximum inductor current ripple, voltage constraints of the circuits implementing the hysteresis band, etc. The first step is to define i_{Cin} from requirements on i_L , PV voltage ripple, or switching frequency (28). Then, K_2 is designed from (29) based on the desired hysteresis band H and i_{Cin} value. Subsequently, constraints in (21) and (22) must be evaluated within the operation range of the PV system,where the maximum reference derivative permissible depends on the parameter K_1 . These expressions together with (34) and (35) form a nonlinear equation system that must be solved by means of numerical methods, e.g., Newton– Raphson, Trust-Region, Levenberg–Marquardt, genetic algorithms, among others. The solution of the equation system givesthe required values ofK_1 andW_n to guarantee the SMC desired behavior.

V. SIMULATION RESULTS

The proposed procedure to analyze and design the SMC for the PV system in Fig. 5 is illustrated in the following conditions. An irradiance operation range within 100 W/m2 $\leq S \leq$ 1000 W/m2 with a maximum continuous irradiance derivative m2, which simulates a transition from the highest irradiance to complete shade in 1 s. The adopted PV module is a BP585 with average parameters i_{SC} = 5 A, and MPP voltages between 16.39 and 18.13 V. The parameters of the dc/dc converter are L = 22.5 μH, C_{in} =

66 μF, C_o = 66 μF, v_b = 29 V, and a PV voltage operation within 10 V $\leq v_{PV} \leq$ 20 V. In addition, the load perturbations generated by a grid-connected inverter consider a grid frequency f_{grid} = 50 Hz and a maximum variation of v_b equal to 34.5%, i.e., 24 V $\leq v_b \leq$ 34.The SMC design considers the following P&O parameters: T_a = 2 ms and v_{MPPT} = 2 V. To ensure the P&O stability, the desired settling time of the PV voltage is set to t_s = 0.5 ms, but many other $t_s \leq T_a$ can be adopted. Concerning practical limitations, the switching frequency must be smaller than 95 kHz, and the implementation of the control action in Fig. 6 is performed using a TS555 integrated circuit, which imposes an hysteresis band H = 1.667 V for a supply voltage V_{cc} = 5 V. The current ripple of the input capacitor is calculated from (28) at the maximum load voltage and MPP voltage obtaining i_{Cin} = 4 A. Then, the magnitude of K_2 is calculated from (29), obtaining K_2 = −0.417 V/A. Subsequently, the equations system formed by (21), (22), (34), and (35) is solved using the *f*solve() function of MAT-LAB with the Trust-Region method, obtaining $K1$ = −0.212 and Wn = 1.0535 × 106 rad/s with a maximum derivative of the reference max

This simulation shows a correct tracking of the P&O reference with the desired setting time ts = 0.5 ms in presence of large load voltage variations of 34.5%. The correct operation of theP&Ois confirmed by the accurate tracking of the maximum PV power available $p$max. The simulation considers a PV array formed by two BP585 panels in parallel, both with an irradiance level of S = 600 W/m2. At t = 10 ms, one of the panels is disconnected to simulate a step-like disturbance of 50% in PV current, and at t = 20 ms, the PV module is connected again.

The results show the accurate tracking of the MPPT and the satisfactory mitigation of the perturbations, which demonstrates the effectiveness of the proposed design procedure. Fig. 8(b) presents a similar simulation but considering a PV array formed by two BP585 panels in series. The PV system operates with a single panel up to t = 10 ms, from that instant, the second panel is connected to illustrate the tracking performance when the optimal PV voltage changes considerably.

Again, the designed SMC enables the P&O to track the new MPP. To illustrate the improvement of the proposed design method over the procedures reported in [15] and [20], the design of the SMC based on Ψ in (6) is contrasted with the design of the controller based on Ψ*iL* in (1), reported in [15], and with the design of the controller based on Ψ*iC* in in (3), reported in [20]. To perform a fair comparison, the linear controllers required for both Ψ*iL* and Ψ*iC* in were designed to provide null overshoot and a settling time equal to 0.5 ms. Fig. 9(a) presents the controllers response to a step change in the reference, where both Ψ*iL* and Ψ*iC* in options do not fulfill the overshoot and settling time requirements.

To provide comparisons in different operating conditions, the three controllers were redesigned for 19 different settling times between 0.1 and 1.0 ms. Fig. 9(b)–(d) compares the settling time errors, overshoots, and energy losses provided by the three options. Those simulations confirm that the design procedure proposed in this paper ensures the required settling time and overshoot, while the design procedures reported in [15] and [20] lead to large errors in both the settling time and overshoot as analyzed in Sections II and III.

Moreover, the inaccurately long settling times provided by both Ψ*iC* in and Ψ*iL* , e.g., 350% to 450% in some cases, could lead to violate the P&O stability condition $Ta \geq ts$. In addition, the longer settling times and overshoots make both Ψ*iC* in and Ψ*iL* produce larger energy losses, 30% to 45% in some cases.

The simulations presented in this section put in evidence the effectiveness of the proposed design procedure, since the SMC based on Ψ provides a correct tracking of MPP, in presence of perturbations in both irradiance level and load voltage, for a wide operation range. Moreover, the simulations also confirm the advantages of the proposed procedure over the design methods reported.

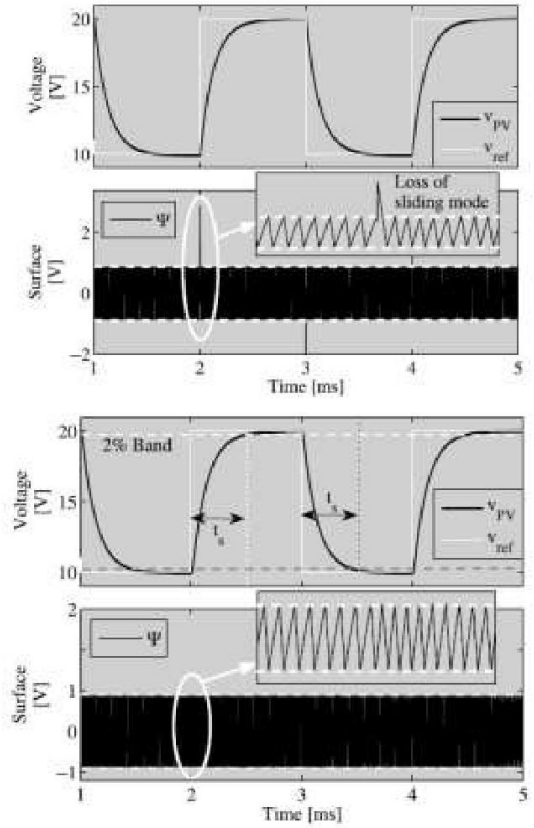

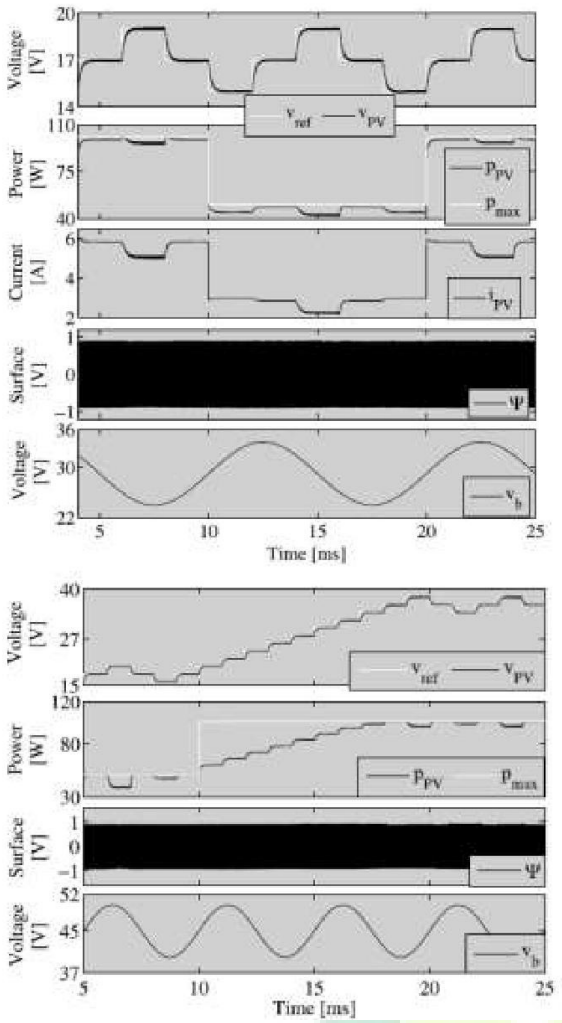

VI. IMPLEMENTATION AND EXPERIMENTAL RESULTS

This section presents experimental validations of the proposed design procedure. The experimental test bench consists in a PV array made of two BP585 modules, a boost dc/dc converter, an electronic load, a DSP device with a MCP4822 digital-to-analog converter (DAC) to implement the P&O as in [7], and a circuit based on operational amplifiers and a TS555 to implement the SMC. The TS555 and all OpAmps (rail-to rail TLC2272 and OPA2350) are unipolar 5-V powered. The structure of the experimental platform is presented in Fig. 10, where the PV panels can be connected in series or parallel depending on the test. Additional switches make possible the connection or disconnection of the PV modules to emulate 50% step-like irradiance transients or to instantaneously change the optimal PV voltage. The converter, PV array, settling time, and P&O parameters are the same ones that are previously adopted for the simulation results; therefore, the SMC parameters $K1$, $K2$, and Wn calculated in Section V hold for the experimental system. The laboratory setup is presented in Fig. 11, which also shows the PC used to program the DSP.

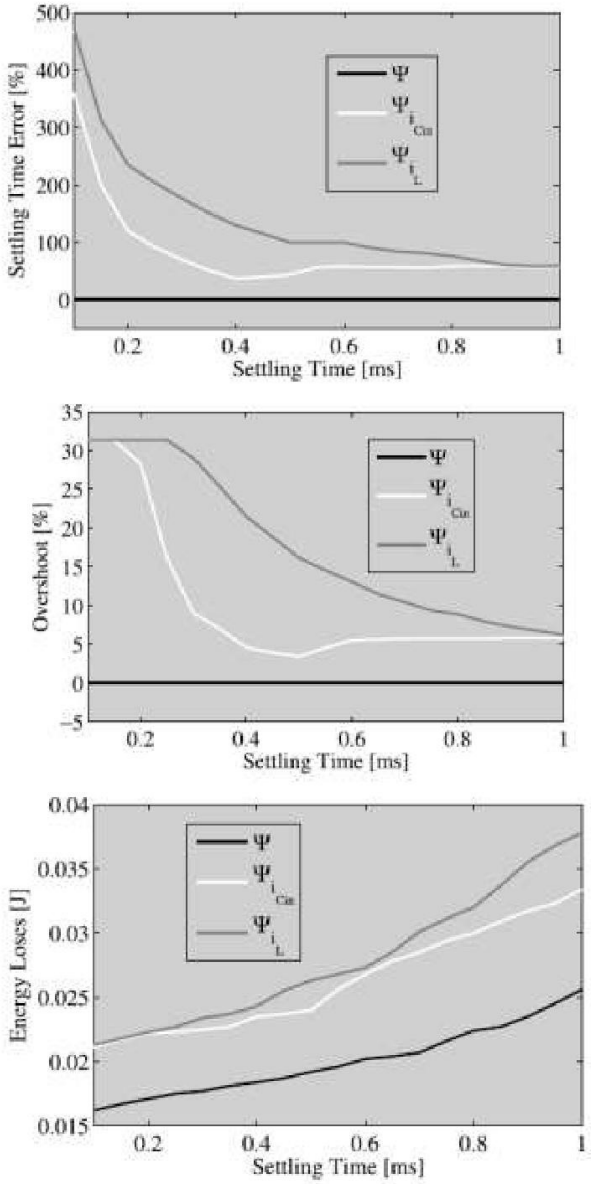

MCP4822 DAC, it is not possible to implement a digital version of the reference filter. Fig. 12(a) also shows the performance of two digital filters designed with shorter sampling times tsF = 1.5 μs and tsF = 0.5 μs, where only the one with tsF = 0.5 μs achieves the desired settling time (0.5 ms), but it requires a DAC nine times faster, i.e., a much costly device.

Another option is to implement a derivative limiter instead of a traditional filter. In this case, the step-like reference provided by the P&O becomes a ramp waveform with slope equal to max dvr e f dt, where the time required by the ramp to reach the reference voltage. Then, the number of steps forming the digital ramp is NRAMP = 1 + tRAMP/tsF . Using the DAC with tsF = 4.5 μs adopted in the experimental platform NRAMP = 1, hence no slope limitation is performed as depicted in the simulations of Fig. 12(b). Such a figure also presents the digital ramps achieved with shorter tsF = 1.5 μs and tsF = 0.5 μs, where the first one provides two steps, while the latter one provides six steps. Again, a much faster DAC is needed, in comparison with the MCP4822, to achieve an acceptable digital ramp. The previous analyses show that the adopted DAC forces the analog implementation of the reference filter. However, faster DACs enable to integrate the reference slope limitation into the digital device used to process the MPPT algorithm.

The proposed procedure for designing the SMCwas validated by reproducing the simulation tests using the experimental platform of Fig. 10; Fig. 13 shows the experimental behavior of the PV system in presence of step commands injected to the reference, similar to the simulations presented in Fig. 7. This test validates the design of the analog filter added to the reference of

the SMC to ensure the system operation inside the sliding band. Moreover, Fig. 13(b) validates the procedure to calculate $K1$, $K2$, and Wn to impose a desired settling time to the PV voltage including the filter effect.

Two additional experiments were made to verify the performance of the complete PV system including the MPPT algorithm: The first one considers a fast change in the irradiance, and the second one considers a fast change in the MPP voltage. In both tests, the electronic load was configured to impose a 100 Hz oscillation at the output port of the dc/dc converter to emulate a disturbance of 34.5% generated by a grid-connected inverter.

In the first case, the PV array is formed by two parallel connected modules. Then, one of those modules is disconnected to emulate a step-like 50% perturbation in the irradiance. Fig. 14(a) presents the experimental waveforms, where the P&O exhibits a stable three-point profile in presence of both the irradiance and load voltage perturbations, which put in evidence the satisfactory performance of the proposed design procedure.

In the second case, the PV array is originally formed by a single module. Then, an additional module is connected in series to produce a fast change on the MPP voltage. Fig. 14(b) presents the results of this experiment, where the P&O accurately tracks the new MPP in presence of the load voltage perturbations, which verifies again the satisfactory performance of the design procedure. Finally, the experimental results presented in this section validate the correctness of the proposed procedure to designthe SMC in agreement with the requirements of the MPPT algorithm.

Its PV voltage tracked the reference provided by an external MPPT with a specified settling time and no overshoot while being insensitive to changes in environmental conditions, such as solar irradiation or PV module temperature, and the 100/120-Hz perturbations in the bulk capacitor voltage linking the boost converter and the cascaded inverter connected to the grid. In the analysis of the selected switching surface, formed by a linear combination of the input capacitor current and the PV voltage error, a single control loop has been considered.

This approach differs from other similar solutions previously reported that used cascade controllers based on inner fast current control loops and outer voltage loops designed after a linearization of the current loop dynamic response. Avoiding the linearization, it is a key feature of the improved procedure because the validity of the analytical expressions is not restricted around an operating point, provided that the sliding regime is not lost. As expected from other solutions, the expression of the equivalent control obtained in the sliding analysis indicated that a low-pass profiler had to be inserted between the MPPT module and the controller input, so that the usually large time derivatives in the MPPT-provided reference voltage were sufficiently limited to avoid losing the sliding regime.

It has been found that instead of the first-order low-pass filter of previous solutions, a second-order critically damped filter provided the same smoothing functionality but with much shorter settling times. While the poorly designed filters of previous approaches caused the controllers to fail in providing the PV voltage responses with no overshoot and the specified settling times required by MPPT, simulation and experimental results showed that the controller is designed following the improved procedure fulfilled correctly all these requirements. The controller parameters were calculated by solving a nonlinear set of equations obtained by combining the filter design equations with the restrictions necessary for the sliding regime to hold in all the PV module and dc/dc converter operating points.

In the simulations and experiments, a SMC with a very simple Variable switching frequency hysteretic modulation was considered. A description of the experimental setup together with a detailed controller implementation based in rail-to-rail OpAmps and the well-known 555 timer, powered by a 5-V uni polar supply, has been provided to help readers in reproducing the experimental results.

Finally, the same detailed analysis and design of SMC can be applied in further developments to PV systems based on other converter topologies such as buck (e.g., battery charges), buck–boost (e.g., module optimizers), inverters (e.g., PV microinverters), among others.

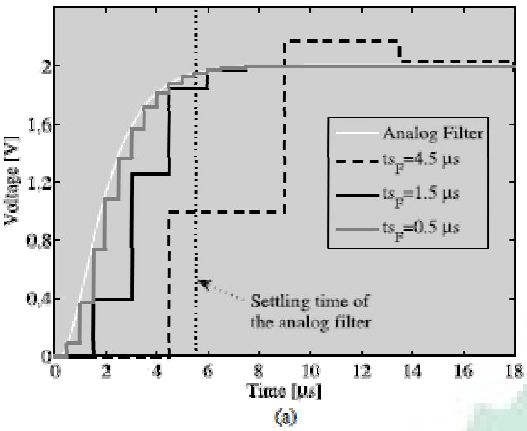

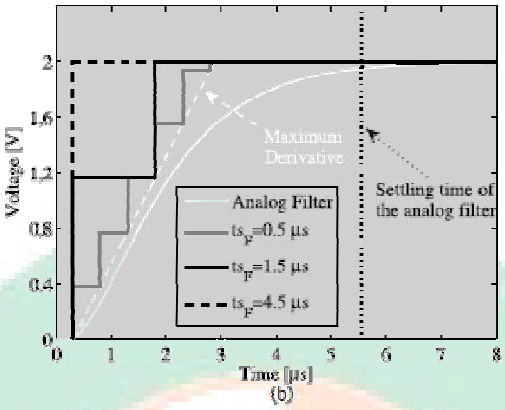

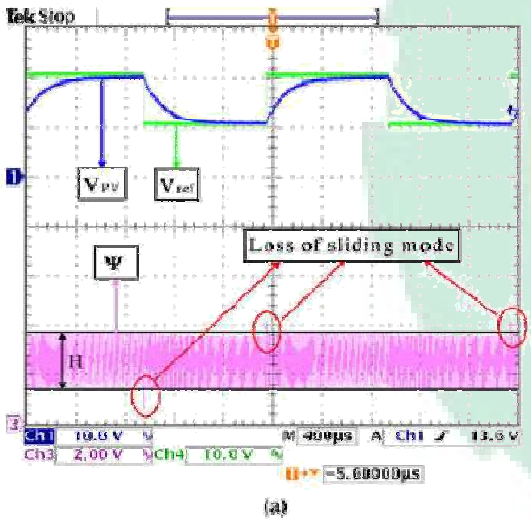

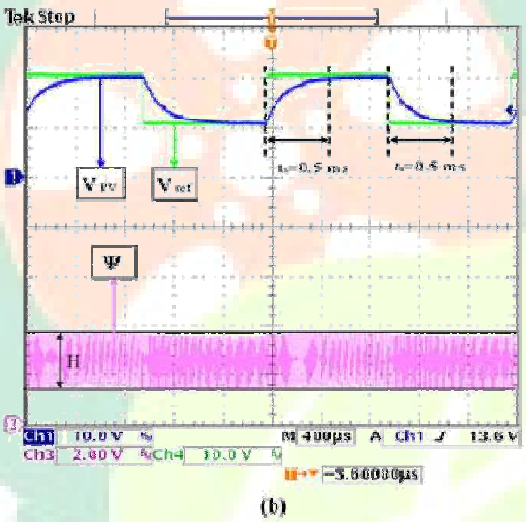

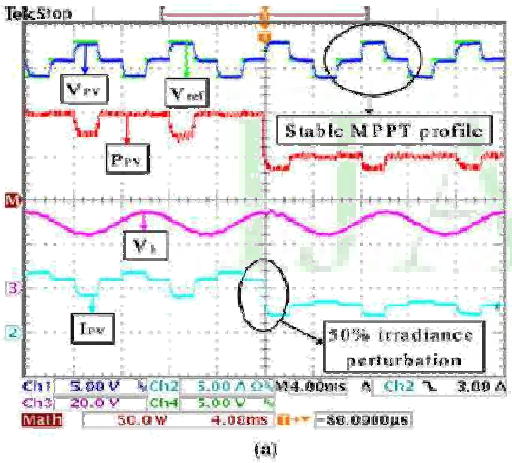

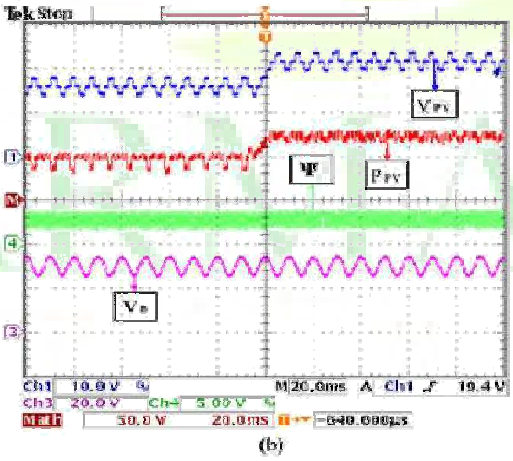

This paper has proposed an improved procedure for designing the SMC of a boost converter in a grid-connected PV system.

REFERENCES

[1] Daniel Gonz´alez Montoya, Carlos Andr´es Ramos-Paja ―Improved Design of Sliding-Mode Controllers Based on the Requirements of MPPT Techniques‖ *IEEE Trans. Power Electron.*, vol. 31, no. 1, pp. 46– 1, Jan. 2016.

[2] E. Koutroulis, K. Kalaitzakis, and N. Voulgaris, ―Development of a microcontroller-based, photovoltaic maximum power point trackingcontrol system,‖ *IEEE Trans. Power Electron.*, vol. 16, no. 1, pp. 46–54, Jan. 2001.

[3] B. Yang, W. Li, Y. Zhao, and X. He, ―Design and analysis of a gridconnected photovoltaic power system,‖ *IEEE Trans. Power Electron.*, vol. 25, no. 4, pp. 992–1000, Apr. 2010.

[4] R. Khanna, Q. Zhang,W. Stanchina, G. Reed, and Z.-H.Mao, ―Maximum power point tracking using model reference adaptive control,‖ *IEEE Trans. Power Electron.*, vol. 29, no. 3, pp. 1490–1499, Mar. 2014.

[5] N. Femia, G. Petrone, G. Spagnuolo, and M. Vitelli, ―Optimization of perturb and observe maximum power point tracking method,‖ *IEEE Trans. Power Electron.*, vol. 20, no. 4, pp. 963–973, Jul. 2005.

[6] C. Konstantopoulos and E. Koutroulis, ―Global maximum power point tracking of flexible photovoltaic modules,‖ *IEEE Trans. Power Electron.*, vol. 29, no. 6, pp. 2817–2828, Jun. 2014.

[7] T. Esram, J. Kimball, P. Krein, P. Chapman, and P. Midya, ―Dynamic maximum power point tracking of photovoltaic arrays using ripple correlation control,‖ *IEEE Trans. Power Electron.*, vol. 21, no. 5, pp. 1282–1291, Sep. 2006.

[8] R. Mastromauro,M. Liserre, and A. Dell'Aquila, ―Control issues in single stage photovoltaic systems: MPPT, current and voltage control,‖ *IEEE Trans. Ind. Informat.*, vol. 8, no. 2, pp. 241–254, May 2012.

[9] T. Esram and P. L.Chapman, ―Comparison of photovoltaic array maximum power point tracking techniques,‖ *IEEE Trans. Energy Convers.*, vol. 22,no. 2, pp. 439–449, Jun. 2007.

[10] N. Femia, G. Petrone, G. Spagnuolo, andM. Vitelli, ―A new analogMPPT technique: Teodi,‖ *Prog. Photovoltaics, Res. Appl.*, vol. 18, no. 1, pp. 28– 41, 2010.

[11] G. Walker and P. Sernia, ―Cascaded dc-dc converter connection of photovoltaic modules,‖ *IEEE Trans. Power Electron.*, vol. 19, no. 4, pp. 1130– 1139, Jul. 2004.

[12] G. Petrone, G. Spagnuolo, R. Teodorescu, M. Veerachary, and M. Vitelli, ―Reliability issues in photovoltaic power processing systems,‖ *IEEE Trans. Ind. Electron.*, vol. 55, no. 7, pp. 2569–2580, Jul. 2008.

[13] A. Trejos, D. Gonzalez, and C. A. Ramos-Paja, ―Modeling of stepup grid-connected photovoltaic systems for control purposes,‖ *Energies*, vol. 5, no. 6, pp. 1900–1926, 2012.

[14] J. Chavarria, D. Biel, F. Guinjoan, C. Meza, and J. Negroni, ―Energybalance control of PV cascaded multilevel grid-connected inverters under level-shifted and phase-shifted PWMs,‖ *IEEE Trans. Ind. Electron.*, vol. 60, no. 1, pp. 98–111, Jan. 2013.

[15] S.-C. Tan, Y. M. Lai, and C. K. Tse, ―General design issues of slidingmode controllers in dc-dc converters,‖ *IEEE Trans. Ind. Electron.*, vol. 55, no. 3, pp. 1160–1174, Mar. 2008.

[16] E. Bianconi, J. Calvente, R. Giral, E. Mamarelis, G. Petrone, C.A. Ramos- Paja, G. Spagnuolo, andM. Vitelli, ―Perturb and observe MPPT algorithm with a current controller based on the sliding mode,‖ *Int. J. Electr. Power Energy Syst.*, vol. 44, no. 1, pp. 346– 356, 2013.

[17] J. Knight, S. Shirsavar, and W. Holderbaum, ―An improved reliability cuk based solar inverter with sliding mode control,‖ *IEEE Trans. Power Electron.*, vol. 21, no. 4, pp. 1107–1115, Jul. 2006.

[18] E. Mamarelis, G. Petrone, and G. Spagnuolo, ―Design of a sliding-modecontrolled SEPIC for PV MPPT applications,‖ *IEEE Trans. Ind. Electron.*, vol. 61, no. 7, pp. 3387–3398, Jul. 2014.

[19] Y. Levron and D. Shmilovitz, ―Maximum power point tracking employing sliding mode control,‖ *IEEE Trans. Circuits Syst. I, Reg. Papers*, vol. 60, no. 3, pp. 724–732, Mar. 2013.

[20] N. Femia, G. Petrone, G. Spagnuolo, and M. Vitelli, ―A technique for improving P&O MPPT performances of double-stage grid-connected photovoltaic systems,‖ *IEEE Trans. Ind. Electron.*, vol. 56, no. 11, pp. 4473– 4482, Nov. 2009.*Electronics*. New York, NY, USA: Kluwer, 2004.